

**Shape Dynamics of Nanobubbles Located on Bunched and Wide Terraces at
HOPG/Water-Ethanol Interface**

Naoki Kameda and Seiichiro Nakabayashi*

Department of Chemistry, Faculty of Science, Saitama University, Saitama 338-8570,
Japan

The time courses of the nanobubbles were investigated at HOPG surface contacting with air-saturated water-ethanol mixed solution. At the high step density surface, the bubbles confined within the narrow bunched terrace, and coalesced to form the elliptic bubble. The final volume of the coalesced bubble was bigger than that of the sum of the individual initial bubbles. On the wider terrace, the volume of the solitary hemispherical bubble changed stochastically and the larger fluctuation accompanied the smaller bubble.

KEYWORDS: bubble, HOPG, fluctuation, mesoscopic, solid liquid interface

*Corresponding author, E-mail address: sei@chem.saitama-u.ac.jp

The interface, where more than a couple of phases contact each other has a different nature from each of the contributing bulk phase. The three phases (gas, liquid and solid) contacting region is important for both of the natural and the artificial functions such as the gas exchange in the lung¹⁾ and the electrochemical reaction on the fuel cell electrode.²⁾ The analysis of the triple phases contacting region requires the specific nano-science and technology that work in the ambient atmosphere, high-pressure gas or liquid. One of the modern topics of these three phase science is the nanobubble, which is a nanometer size bubble appearing on the hydrophobic solid surface contacting with gas containing liquid.^{3,4)} The nanobubbles are certainly the ubiquitous phenomena, but the existence of the bubbles has been proved quite recently.^{3,4)}

For the non-UHV surface experiments, the practical difficulty is the preparation of the clean and well-defined surface. In order to overcome this difficulty, highly oriented pyrolytic graphite (HOPG) was used since the freshly cleaved surface provides the well-defined substrate.⁵⁾ The AFM image of HOPG obtained in air was shown Fig. 1(a), where the cross section was plotted below. The c-axis lattice constant is 0.67nm as shown in Fig. 1(b), and then one, two, two and two atomic steps separated the ①-⑤ terraces in the image, respectively. The terraces located between the step lines are atomically flat and chemically homogeneous. The widths of the terrace i.e., the density of the step lines were varied by the cleaving procedure. The AFM used was Nanoscope III (Veeco) operated under the tapping mode (TM-AFM) with an extra Q-control circuit (NanoAnalytics).

The two kinds of HOPG surfaces (with the high and low step line density; 5 and 1

lines /1 μm , respectively) were contacted with air-saturated water-ethanol mixture (1:1 in the volumetric ratio) after flashing the surface by pure ethanol. As shown in Fig. 2(a), the elliptic bubbles appeared along the step edge on the bunched terrace at the high step density surface, where the cross section along the dotted line was shown above the image. Two, one and one atomic steps separated the ①–④ terraces, respectively. However, as shown in Fig. 2(b), the solitary hemispherical bubble was observed on the wider terrace at the low step density surface, where the cross section was shown below the image. Only mono atomic trench ② was observed among ①–③ regions. The density of the bubble in Fig 2 (a) was 3 bubbles/ μm^2 . This bubble density was 10 times higher than that in Fig 2 (b), where the density was 0.3 bubble/ μm^2 . No bubble was observed in pure ethanol at both of the surfaces. Then, the ethanol-flash erases the bubbles and resets the initial conditions. The observation cycles; the ethanol-flash, the introduction of the air saturated water-ethanol and the TM-AFM imaging, were repeated.

The time evolution of the bubbles at the high step density surface was demonstrated in Fig. 3. The cross sections along the dotted line were shown below. Two, one and one atomic steps separated the ①–④ terraces, respectively. All of the bubbles are confined within the narrow terraces between the step edges. Many of the coalescences events between neighboring bubbles in the same terrace were observed but not between the bubbles located in the neighboring terraces. In Fig.3, the typical two events were shown in the circles (i) and (ii). The time course of the motions of the bubbles was demonstrated in Fig. 3(a)-3(c). The intervals between (a) -(b) and (b) -(c) are 500 and

1500 s, respectively. The shapes of the bubbles before and after the coalescence are quasi-hemispherical and elliptic with the long axis parallel to the step line, respectively. In case (i), the height of the bubbles are around 2.5 nm, and the diameters are 210 x 210 nm and 200 x 320 nm before and after the coalescence, respectively. The bubble coalescence requires the couple of the bubbles located on the same terrace and the distance is so close that the bubble deformation can make a bridge.

The changes in the volume through the coalescence were plotted in Fig. 4 (a) and (b), where the two typical examples appearing in (i) and (ii) in Fig. 3 were shown, respectively. The temporal error bars are due to the time needed to complete the imaging. The spatial error was estimated by the repeated measurements of the standard sample, the mono-atomic step of HOPG in the liquid. The volumetric error bars were smaller than the circles in the plots. The Ostwald ripening drives the coalescence.⁵⁾ The surface energy γ_{LG} (the macroscopic value of the ethanol-water mixture is 2.8×10^{-2} J/m.^{1,7)}) compress the bubble and this additional internal pressure ΔP (Laplace pressure) is given by $\Delta P = 2\gamma_{LG}/R$, where R is the radius curvature of the bubble.^{6,8,9)} The smaller bubble has the larger Laplace pressure. Then, when the two bubbles are connected by the bridge, the smaller bubble is hydro-dynamically merged into the larger one. The formation of the bridge is owing to the interplay between the stochastic and/or the tip induced bubble deformation. In Fig. 4(a), the smaller bubble (the initial volume was $8.0 \times 10^4 \text{ nm}^3$) was merged into the bigger bubble (the initial volume was $2.4 \times 10^5 \text{ nm}^3$), and the final volume of the coalescent bubble ($7.3 \times 10^5 \text{ nm}^3$) was almost two times larger than the sum of the initial individual volumes. In both of the cases (a) and

(b), the volumes are fluctuating at the initial induction periods. At just before the drastic change in the volume, the smaller bubbles are merged into the larger bubbles. The final volumes of the coalescent bubbles are always bigger than the sum of the contributing individual bubbles.

The volume of the solitary hemispherical bubble on the terrace appearing in Fig. 2(b) was stochastically varied. The typical volumetric time evolutions of the three different bubbles were shown in Fig. 5(a)-(c). The obtained stochastic deviation was certainly larger than the measurement errors, which were estimated by the same procedure in Fig.4. The average volumes of the bubbles, V_o were 8.7, 7.7 and 3.7 x 10⁴ nm³ for Fig.5 (a)-(c), respectively. Apparently, the life of a solitary bubble was over hours. Then, the steady state of the concentration of the gas molecules is achieved in between the bubble and the surrounding water-ethanol mixture. The balance of the couple of the gas fluxes sustains the steady state, where J_{in} and J_{out} are the flux from the water-ethanol mixture into the bubble and that of the reverse direction, respectively. The temporal average of the fluxes are equal to sustain the nanobubble, i.e., $\langle J_{in} \rangle = \langle J_{out} \rangle$. Because of the mesoscopic size of the bubble, at a specific timing, the couple of the fluxes are not necessarily equal; $[J_{in}]_t \neq [J_{out}]_t$. This unbalance induces the fluctuation of the volume of the bubble. The magnitude of the fluctuation δ is defined as

$$\delta = \sqrt{\sum_{i=1}^N \left(\frac{V_i - V_o}{V_o} \right)^2},$$

which is shown at the upper right of Fig.5. As the decrease of

the average volume V_o , δ increased, which reasonably demonstrates that the fluctuation increases as decrease of the size of the system.

This article revealed the coalescence and stochastic behavior of nanobubbles on the well-defined surface of HOPG. All of the results are qualitatively explained by the mesoscopic nature of the nanobubbles. The nanobubble is expected to be a good example for the mesoscopic super-structure in the soft matter surface science.

Reference

- 1) Y. Y. Zuo, R. Gitiafroz, E. Acosta, Z. Policova, P. N. Cox, M. L. Hair, and A. W. Neumann: *Langmuir* **21** (2005) 10593.
- 2) B. Conway: in *Impedance Spectroscopy*, eds. E. Barsoukov, J. R. Macdonald (Wiley, New Jersey) Chap. 4.5.3, p469.
- 3) N. Ishida, T. Inoue, M. Miyahara, and K. Higashitani: *Langmuir* **16** (2000) 6337.
- 4) J. W. G. Tyrrell, and P. Attard: *Phys. Rev. Lett.* **87** (2001) 176104-1.
- 5) X. H. Zhang, X. Zhang, J. Sun, Z. Zhang, G. Li, H. Fang, X. Xiao, X. Zeng, and J. Hu: *Langmuir* **23** (2007) 1778.
- 6) S. A. Safran: *Statistical Thermodynamics of Surfaces, Interfaces, and Membranes* (Perseus Book, Massachusetts, 1994) Chap.2 and 4.
- 7) C. J. West, and C. Hull: *International Critical Tables of Numerical Data, Physics, Chemistry and Technology* (McGraw-Hill Book Company, Inc., New York and London, 1993) p467.
- 8) M. Conti, B. Meerson, A. Peleg, and P. V. Sasorov: *Phys. Rev. E* **65** (2002) 046117-1.
- 9) G. Andreatta, L. Lee, F. K. Lee, and J. Benattar: *J. Phys. Chem. B* **110** (2006) 19537.

Figure Captions

Fig. 1 Image of freshly cleaved HOPG in air (a) with the cross section. The differences in the heights are 0.34, 0.75, 0.69 and 0.60 nm for the steps between ①–②, ②–③, ③–④ and ④–⑤ terraces, respectively. Schematic representation of the surface structure (b) with the c-axis lattice constant of 0.67nm.

Fig. 2 Typical images of the elliptic bubble confined on the bunched terrace (a). The differences in the heights are 0.77, 0.38 and 0.37 nm for the steps between ①–②, ②–③ and ③–④ terraces, respectively. The solitary hemispherical bubble on the wider terrace (b). The differences in the heights are 0.38 and 0.38 nm for the steps between ①–② and ②–③ terraces, respectively.

Fig. 3 Time evolved images through the bubble coalescence within the bunched terrace. The time interval between (a) and (b), and that between (b) and(c) are 500 and 1500 s. The coalescences are proceeding in the regions (i) and (ii). The differences in the heights are 0.77, 0.38 and 0.37 nm for the steps between ①–②, ②–③ and ③–④ terraces, respectively. The red and black lines in the cross section of (a) are corresponding to the nanobubble and the underlying substrate, respectively.

Fig. 4 Temporal changes in the volumes through the bubble coalescences. The plot (a) and (b) are corresponding to the regions (i) and (ii) in Fig. 3, respectively.

Fig. 5 Temporal fluctuations in the volume of the solitary hemispherical bubbles on the wide terrace. The average volumes of bubbles (a), (b) and (c) are 8.7, 7.7 and $3.7 \times 10^4 \text{ nm}^3$, respectively. The fluctuation δ are 0.39, 0.34 and 0.48 for (a) to (c), respectively.

Figure 1

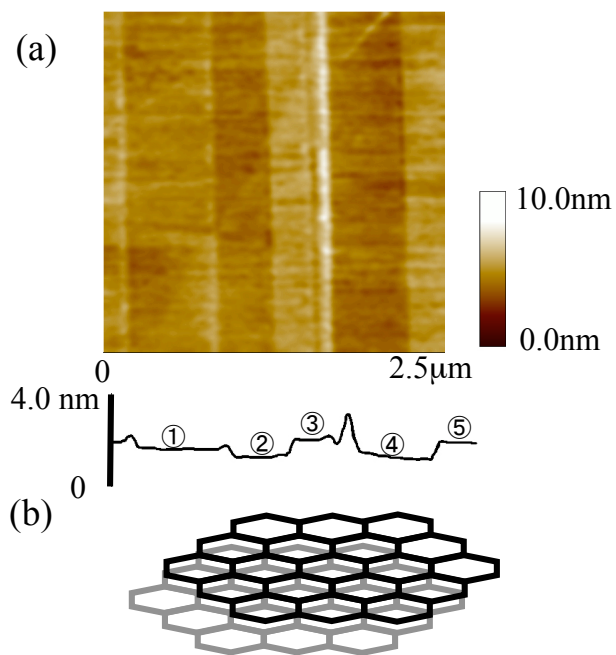


Figure 2

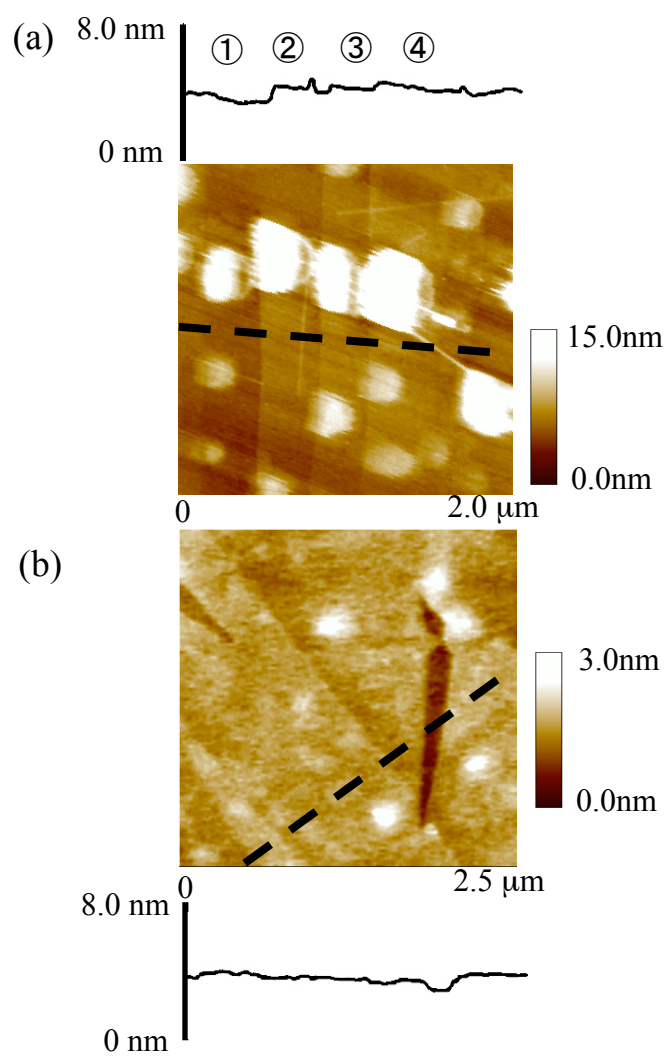


Figure 3

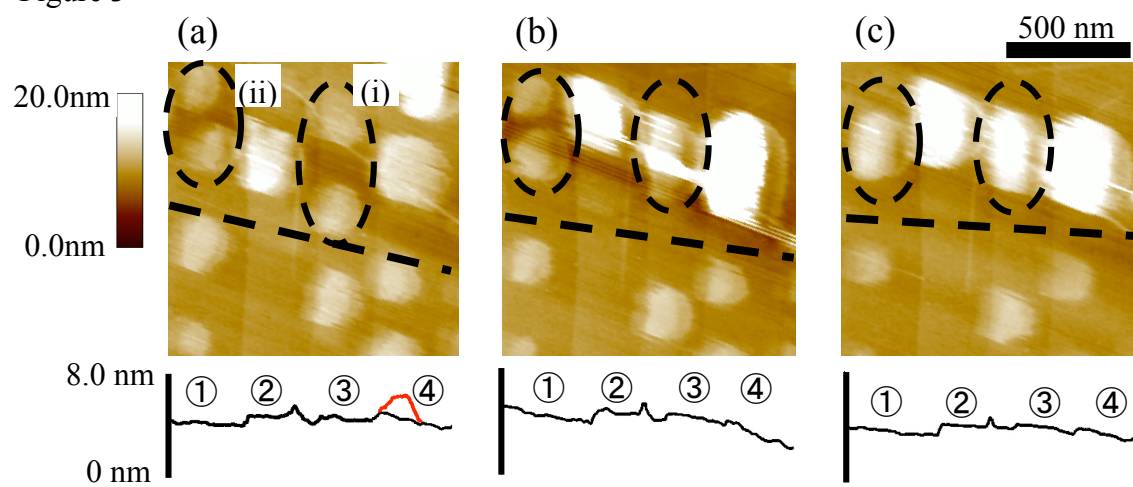


Figure 4

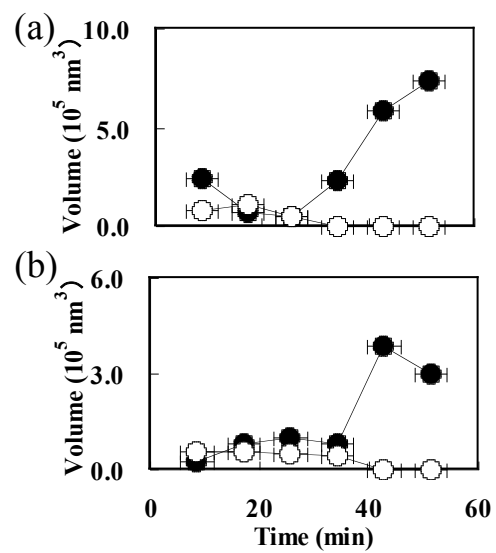


Figure 5

